
Characterization of Aliwal North Hotspring in the Eastern Cape Province of South Africa, using Magnetic, Electromagnetic and Radiometric Methods

C. Baiyegunhi¹, N. W. Mupandawana¹, T. L. Oloniniyi² and O. Gwavava¹

¹Department of Geology, Faculty of Science and Agriculture, University of Fort Hare, Private Bag X1314, Alice, 5700, Eastern Cape Province, South Africa

²Department of Geology and Mining, Faculty of Natural and Applied Sciences, Nasarawa State University, Keffi, Nasarawa State, Nigeria

ABSTRACT

Magnetic, electromagnetic and radiometric survey were conducted along two profile lines that traverse Aliwal North spa using two G-859SX portable cesium vapor magnetometer, EM34-3 terrain conductivity meter and a RS-125 spectrometer, respectively. This was undertaken in order to characterise Aliwal North hot spring by revealing magnetic signatures, buried conductive bodies and determine the concentration/relative abundance of radioactive elements, like U, K and Th (in cpm, ppm and %). The magnetic result reveal signature with amplitude of about 0.4 nT, which is inferred to be a real feature extending to depth. The EM result shows major anomaly in the southeastern part of the study area. This anomaly is associated with rocks with high conductivity and occurring to a depth of about 30 m through which the highly mineralized hot water could have migrated to the surface. There is no traceable recent volcanic activity in the area and due to the deep seated faults in the survey site, it was inferred that Aliwal thermal spring is of meteoric origin and the source of the heat is due to the deep circulation along the major fault zones. The radiometric result reveals that thorium is the most abundant radioelements with concentration that is less than the world average hazardous threshold (7.4 ppm). The concentration of the radioactive elements is relatively low and acceptable for groundwater; however it could be harmful to humans' health, as well as animals when exposed to the radiation or consumed over a long period of time.

Keywords: *Magnetic, electromagnetic, radiometric, hot spring, groundwater, Aliwal North*

I. INTRODUCTION

Groundwater is the major source of water in the Republic of South Africa especially in water-scarce area such as Aliwal North where people fetch or get water from groundwater discharge points (springs). A total of about 74 hot springs are known in South Africa (Figure 1; Table 1) cutting across the entire the country (Yibaset *al.*, 2011). The occurrences of these hot springs are not restricted to a particular geology but they are usually seen in locations that has high rainfall as well as existence of deep crustal faulting. Yibaset *al.* (2011) stated that, no exploration boreholes have been drilled in South Africa for the purpose of determining origin, geothermal heat flow, and source as well as the circulation pattern of the source of heat. However, geothermal heat flow has been measured from some boreholes that were drilled for other purposes. Presently, the maximum measured surface temperature of the hot springs is seen at the Siloam hot spring which is about 70 °C. Thus there is low possibility of generating electricity from hydrothermal source; however, research is still ongoing to determine the possible alternative means of power generation.

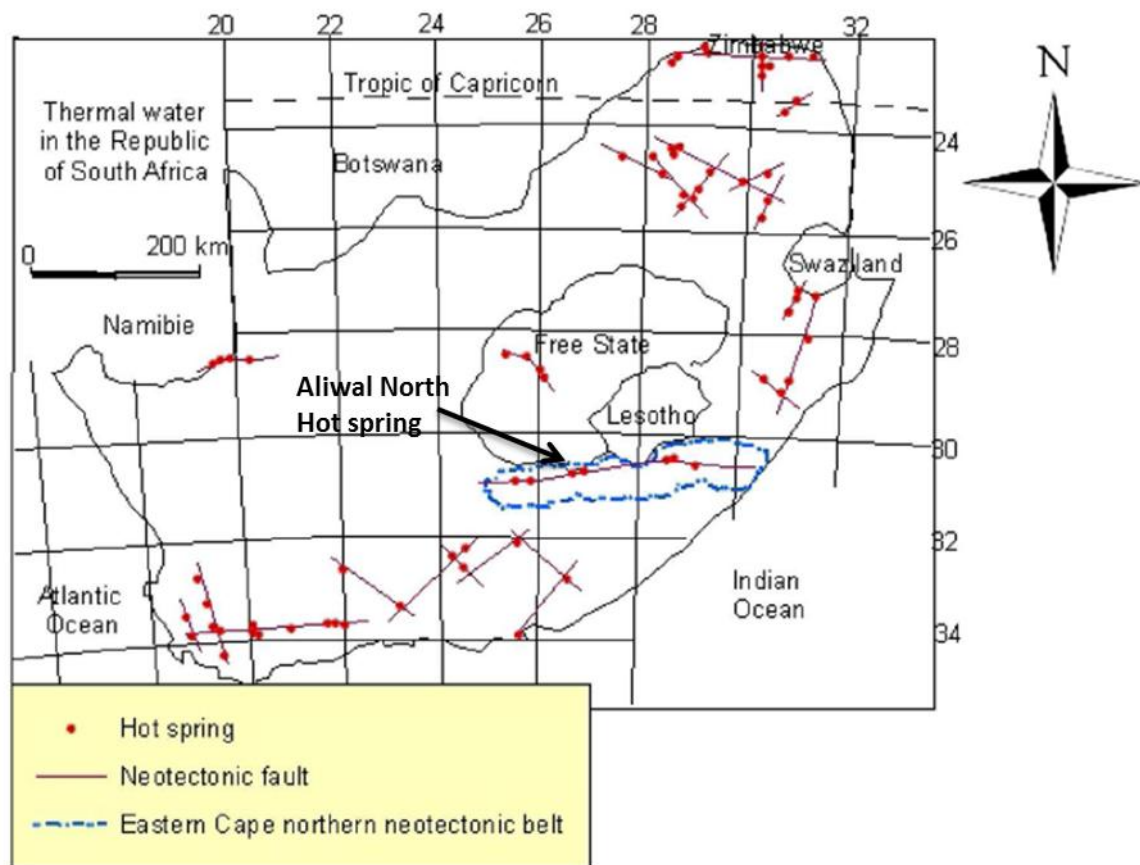


Figure 1 Map showing location of hot springs in the South Africa, neotectonic fault and the Eastern Cape northern neotectonic belt (Madi, 2014).

Table 1 Distribution of hot springs and Boreholes per Province (Olivier *et al.*, 2008)

Province	Kent, 1949			Boekstein, 1998; Hoole, 2001
	Springs	BHs	Total	Developed
Western Cape	14	1	15	9
Northern Cape	4	-	4	1
Eastern Cape	10	3	13	2
KwaZulu-Natal	5	-	5	4
Free State	4	4	8	4
North-West	-	-	-	1
Mpumalanga	13	-	13	3
Gauteng	1	-	1	1
Limpopo	23	1	24	10
Total	74	9	83	35

Aliwal North hot spring is associated with fractured and fault zones (Figure 1) through which the dolerite dykes (groundwater localizers) intruded the sandstones of the Tarkastad Subgroup at about 180 Ma. The spring is not well developed, it has a temperature of about 37 °C and mostly used for washing clothes, bathing and medicinal purposes to cure rheumatism and other related diseases (Hartnady, 2005). Hobday (1978) emphasized on the need of detailed geophysical investigations of contacts between the lithological subdivisions of the Karoo Supergroup in order to characterize and ascertain the origin of the thermal springs in the Karoo Supergroup.

Recently, many of these contacts between the lithological subdivisions have been studied and documented but some areas such as Eccca – Beaufort contact, Beaufort–Molteno contact, and Burgersdorp–Molteno contact are still understudied or difficult to characterise in terms of origin and associated geological structures of the thermal springs. The Molteno-Burgersdorp contact is believed to be defined by an unconformity in which the deposition is preceded by an erosional period but Visser *et al.* (1984) proposed that the Molteno – Burgersdorp contact is conformable, but no absolute date is known for the Burgersdorp and the Molteno Formations. Aliwal North hot spring serves as a target for groundwater exploration, which makes Aliwal North to be regarded as a potential source of groundwater since no detailed geophysical surveys have been carried out previously in Aliwal North, the occurrence and movement of groundwater is unpredictable or complicated. Therefore, it is very important to characterize Aliwal North spa as exploration targets using the magnetic, electromagnetic and radiometric.

1.1 Location of the study area

Aliwal North spa is located in the town of Aliwal North which lies on the border between the Free State and Eastern Cape Province of South Africa. The study area extends from longitudes 26° 42' 52" E to 26° 43' 06" E and latitudes 30° 42' 49" S to 30° 42' 50" S (Figure 2). The town covers an area of about 169580 km² with a population of 6,906,200 people and geographically situated between the Western Cape and KwaZulu-Natal province, the northern part leads to Bloemfontein through the General Hertzog Bridge and to the south-west, the Kramberg raises to about 2,000 m above the sea level (Hartnady, 1985). The climatic condition of the Eastern Cape is a mixture of the climatic condition of the Western Cape and KwaZulu-Natal, it which get very wet gradually from the west to the east part of the province (Hartnady, 1985).

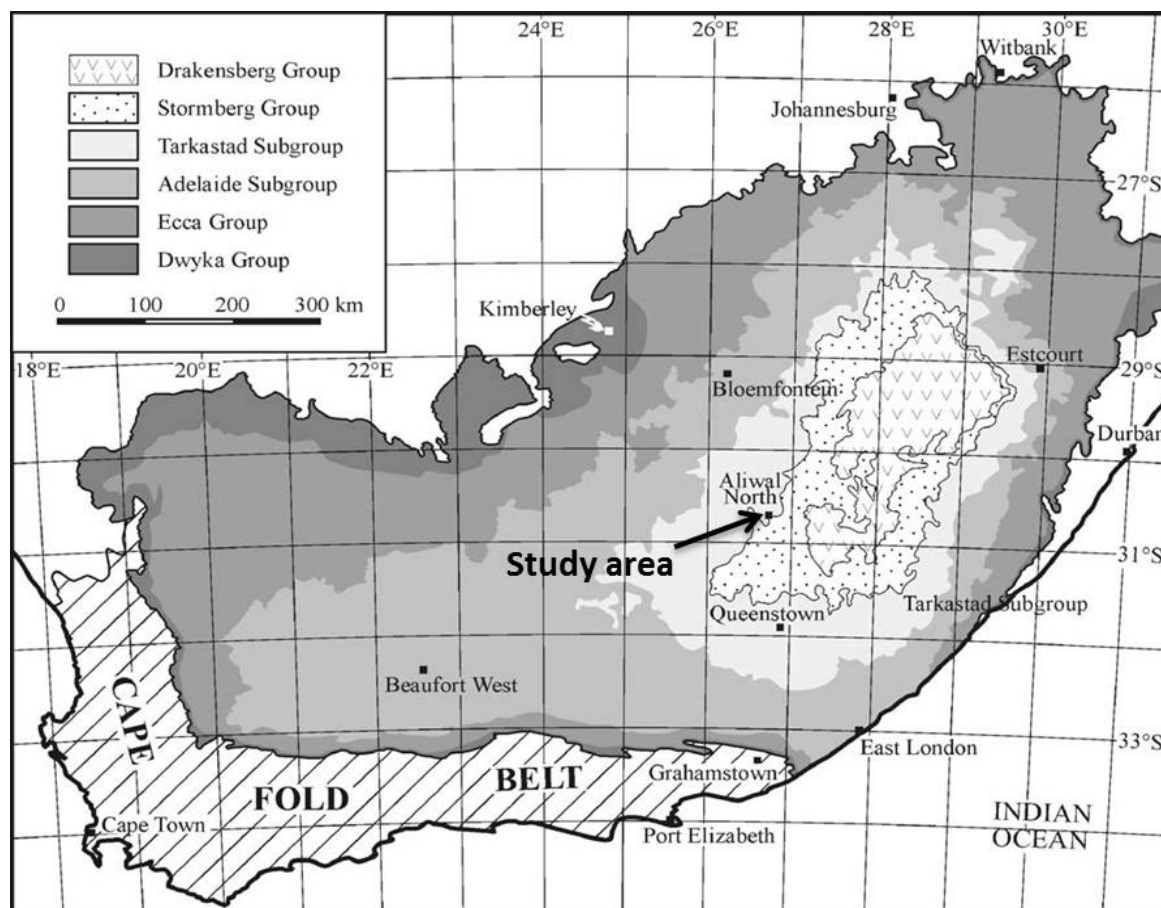


Figure 2 Geological map showing the study area (Catuneanu and Elango, 2001).

1.2 General background

Aliwal North belongs to the Tarkastad Subgroup in the Beaufort Group which is a fluvial environment (Figure 2; Table 2). The Beaufort Group is stratigraphically subdivided into the Adelaide and the Tarkastad Subgroups (Johnson, 1976; Tordiffe, 1978; Visser and Dukas, 1979; SACS, 1980; Catuneanu and Elango, 2001). The Adelaide Subgroup forms the lower part of the Beaufort Group and consists of the Koonap, Middleton and Balfour Formations. The Tarkastad Subgroup where the study area belongs; forms the upper part

of the Beaufort Group and consists of the Katberg and Burgersdorp Formations which are restricted to the southern margins of the Karoo Basin from south of Queenstown to north of Aliwal North (Rubidge, 1995; Hancox and Rubidge, 2001).

Table 2 Lithostratigraphy of the Beaufort Group in the Eastern Cape Province of South Africa (After, Johnson *et al.*, 2006).

GROUP	SUBGROUP	FORMATION	MEMBER	LITHOLOGY	DEPOSITIONAL ENVIRONMENT	
Beaufort	Tarkastad	Burgersdorp		Mudstone, Sandstone, Shale	Fluvial	
		Katberg		Sandstone, Mudstone, Shale		
	Adelaide	Balfour	Palingkloof			Mudstone, Sandstone, Shale
			Elandsberg			Sandstone, Siltstone
			Barberskrans			Sandstone, Khaki Shale
			Daggaboersnek			Shale, Sandstone, Siltstone
			Oudeberg		Sandstone, Khaki Shale	
	Middleton		Shale, Sandstone, Mudstone	Transitional (Deltaic)		
	Koonap		Sandstone, Mudstone			

The Koonap Formation consists of alternating sequence of sandstone and mudstone. It is the base of the Adelaide Subgroup in the lower vicinity of the Beaufort Group and has lithological variation similar to those of the overlying Middleton and Balfour Formations. It has a total thickness of about 1300 m (Johnson, 1976; SACS, 1980). The Middleton Formation has a maximum thickness of about 1500 m and consists predominantly of mudstone with subordinate shale and sandstone (Johnson, 1976). It is essentially a non-marine and siliclastic succession that was deposited in meandering rivers and their extensive environments (flood plains, lakes and ponds). The lithology of the overlying Balfour Formation is dominated by sandstone interbedded with mudstones and it represent a fully succession of Late Permian - Early Triassic age. The total thickness of up to 2150 m was measured around the Fort Beaufort area (Johnson, 1976; SACS, 1980), but Visser and Dukas (1979), working further west of the study area measured about 650 m, thus indicating thickening towards the south east.

Generally, the prevailing climatic condition in South Africa is warm, thus a temperature of 25 °C is use as standard in distinguishing between hot springs and cold springs (Yibas *et al.*, 2011). According to Kent (1949), South Africa's spring is classified into warm (25- 37 °C), hot or hyperthermic (38-50 °C) and scalding (50 °C). It was earlier believed that highest flow rate is associated with the hottest spring, which is not always true because no basis has been given for that (debateable). Hartnady (2005) disagree with the assumption that the hottest springs are those with the highest flow rates. They explained that the occurrence thermal spring temperature reveals the relationship/interaction between advective and conductive movement of heat in the host aquifer system. The aquifer permeability is the key factor since it controls the flow velocity which is proportional to the heat rate; where the groundwater flow velocities/permeability are low and heat transport is dominantly conductive. These conditions usually result in low temperature of the spring (about 25 °C). In rocks where the permeability is high, with high flow velocities and advective transport of heat is dominant, it results in large volume of circulating water leading to high temperature of the spring (38-50 °C). The warmest springs usually occur for an intermediate range of permeability which is the most common type of thermal springs in South Africa (Aliwal North spa) with temperature of (25-37 °C) and when the temperature of the thermal spring is very high (> 50 °C), it is referred to as a scalding thermal spring.

Geothermal springs can be used for different purposes but their uses depend on the temperature of the thermal spring, flow rate, chemistry as well as other economic factors such as the accessibility to the thermal spring, ownership of the resource, distance to a potential user, and environmental limitations. These determine whether the thermal spring is suitable for either electric power generation or direct utilization such as direct

heating of different forms, space heating leisure, spas, aquaculture, floriculture, green house and medicinal purposes (cure rheumatism and related diseases). A thermal spring can experience changes in its features due to local or regional events that affect the source or flow path, the heat source, thermal characteristics along the subsurface flow path, weather pattern and the fractured rock through which the fluid moves to the surface. The hot fluid may either come from a magmatic hydrothermal system or non-magmatic hydrothermal system. In magmatic hydrothermal system, the rock is heated up by the magma which in turn heats up the deep circulating water while in a non-magmatic hydrothermal system; the rock is heated by geothermal gradient which results in thermal water and quickly return to the Earth's surface through the created fractures. Three main components are required for the formation of a hydrothermal system. These include water, heat and permeability in which water can flow to the surface or near the surface, the water that recharge the Aliwal spa is far (up to tens of kilometres) from the discharge and got their source from rainfall, snowmelt, rivers, and lakes which form most of hydrothermal fluids and reaches depth of several kilometres. Hydrothermal systems are found in different geological environments such as hydrothermal vents, sedimentary basins, epithermal to magmatic-hydrothermal ore-forming environments, this environment shows different chemical compositions and fluids flow path.

Donald *et al.* (1992) proposed that most hot springs in the world are linked with waning stages of volcanic activity. There can be changes in thermal spring features due to local or regional events that affect the source or flow path, the heat source, thermal characteristics along the subsurface flow path, weather pattern (climatic change) and the fractured rock through which the fluid move to the surface. The hot fluid move through fractures in the rock creating permeability, the pores may be interconnected allowing the flow of the fluids which are recharged to the surface by the infiltration of rainwater or snowmelt and underground water circulating near magma at great depth or driven by pressure or density giving rise to a spring. The hot fluid may either be from a magmatic hydrothermal system or non-magmatic hydrothermal system. In magmatic hydrothermal system, the rock is been heated up by the magma which in turn heat up the deep circulating waters while in a non-magmatic hydrothermal system, the rock is heated by geothermal gradient (temperature with depth) which results in thermal water and quickly return to the Earth's surface through the created fractures (permeability).

II. MATERIALS AND METHODS

Fieldwork was conducted over a period of time using three geophysical techniques that includes; the magnetic, electromagnetic and radiometric method. The survey was carried out in an outer zone from the hot spring due to the absence of outcrops, only one weathered greyish mudstones was seen outcropping to the surface. The three geophysical methods were employed to allow comparison of the results and to increase the confidence or degree of accuracy of the data since magnetic field dies out with time and the actual age can be determined using the abundance of the radioactive elements obtained from the radiometric survey.

2.1 Instrumentation and technique of magnetic survey at Aliwal North spa

The ground magnetic survey was conducted along two survey lines (L1 and L2) in Aliwal North Spa using two G-859SX portable cesium vapor magnetometer (movable and non-movable magnetometer). The magnetometer uses the Novatel Smart Antenna™ GPS for capturing positions automatically while collecting data in almost 5 different separate survey files, the non-volatile RAM of the magnetometer can record data for 8 to 12 hours at the maximum rate of 5 Hz and operate in the range of 17,000 nT to 100,000 nT, noise level of (0.02 nT, gradient tolerance of 0.05 nT/inch (20,000 nT/m) and temperature drift of (0.005 nT/°C and sensitivity of 0.03 nT at 0.2 sec cycle rate. The non-movable magnetometer was mounted in a quiet place within the survey area (base station) to monitor diurnal variations and the movable magnetometer was carried by the operator, which takes the total magnetic field as the operator walks along the survey lines (L1 and L2). The movable G-859SX portable cesium vapor magnetometer was set up in way that it takes reading at every 2sec, mounted on the operator as depicted in Figure 3 and measurements commenced along lines (L1 and L2). At the end of the survey, the stored data was processed and downloaded into the laptop with the use of MagMap 2000 software to allow for further data processing/reduction.



Figure 3 Magnetic survey using G-859SX portable caesium vapor magnetometer.

2.2 Instrumentation and technique of electromagnetic survey at Aliwal North spa

The instrument used for electromagnetic survey is the EM34-3 terrain conductivity meter. It consists of a transmitter and a receiver coil that works with different frequencies (0.4 kHz, 1.6 kHz and 6.4 kHz), using a self-contained dipole transmitter as the source and a self-contained dipole receiver as a sensor with a measurement accuracy of $\pm 5\%$ at 20 mS/m. The instrument noise level is less than 0.2mS/m and can operate in the temperature range of -40°C to $+50^{\circ}\text{C}$. The survey was carried out along the survey lines using three coil spacing of 10 m, 20 m, and 40 m since the depth of exploration depend on the coil spacing (transmitter and receiver) and the orientation of the coils. The horizontal mode (vertical coplanar) was measured for Line 1 and Line 2 using 10 m, 20 m, and 40 m coil spacing, respectively (see Figure 4). The EM34-3 is very sensitive to both vertical and horizontal geological anomalies and works with a frequency of 6.4 kHz at 10 m coil separation, 1.6 kHz at 20 m coil separation and 0.4 kHz at coil spacing of 40 m. The EM34-3 terrain conductivity meter was used to measure the apparent conductivity of the ground in milliSiemens/meter (mS/m). The survey was performed by three operators, the first operator carried the transmitting coil, transmitter and hold the start point or edge (tip) of the wire (40 m), the second operator carried the receiving coil, receiver, and the end point or edge (the other tip) of the wire (40 m), and the third operator carried a GARMIN-10 GPS, a field notebook for recording the GPS location, the conductivity value on the receiver at every station (e.g. 40 m) which is the distance between the first operator (transmitter) and the second operator (receiver). The technique used is called the "stop and go" and it takes a rectangular shape, the measurements start along a line and end along a line that intersects the start line. To start taking the measurement, the first operator with the transmitter and a coil stands at the starting point and the second operator with the receiver and the second coil stand 40 m away from the transmitter along the base line, both the transmitter and the receiver are switched on and the coil is aligned (vertically) to each other such that an electromagnetic field is generated and received by the receiver. The measurement is taken after balancing the receiver on the graduation of the measuring meter, reading is taken and recorded at every 40 m, the GPS value at the point is also taken and recorded, then the first operator carrying the transmitter and the transmitting coil now move to the point where the receiver was before which is 40 m away from the start point, and the second operator carrying the receiver and the receiving coil now move 40 m further away along the line and both the transmitting and the receiving coils are aligned (vertically) to each other and the reading was taken from the receiver and recorded, the GPS value was also taken and recorded. The procedure as above was carried out and recorded when the distance between the transmitter and receiver were 10 m and 20 m, respectively.



Figure 4 Electromagnetic survey using EM34-3 terrain conductivity meter.

2.3 Instrumentation and technique of gamma ray survey at Aliwal North spa

The portable RS-125 gamma ray spectrometer was used to determine the spatial distribution of three radioactive elements (potassium-K, thorium-Th and uranium-U) at Aliwal North spa. It consists of a detector and analyser, the detector detects or senses gamma rays while the analyser analyses the signal and displays the result. The spectrometer uses a Sodium-Iodide crystal to detect the radioactive elements (K, U, and Th) with an integrated spectrometer system that measures the total amount of the incoming gamma radiation which lies above a particular energy threshold and present the data used for analysis. The survey mode, scan mode, and assay mode are the three operational mode buttons on the spectrometer, which can be easily identify and press by the operator, the assay mode was used for the survey and it gives the concentration of the radioactive elements in percentage (%), parts per million (ppm) and counts per million (cpm). The RS-125 gamma spectrometer uses an external GPS that is connected via bluetooth to automatically capture locations at each reading and stabilizes automatically on the natural occurring radioactive elements (K, U and Th). The instrument takes reading every 11 seconds and can operate in a range of temperatures between -20°C to $+50^{\circ}\text{C}$. The RS-125 gamma ray spectrometer was set up and mounted in the same manner as the magnetic method (Figure 4).

2.4 Data processing and retrieval

Data processing and retrieving was done with the use of MagMap 2000 software, it analyses and process the data from the geophysical instrument (magnetometer, RS-125 spectrometer and EM34-4) and allows for positional modification on the survey data. The operator created a STN file and selected the ASCII data download using RS-232 with MagMap 2000. The downloaded binary data was stored in a binary file with the extension BIN on the laptop. The downloaded file was unzipped using the WinZip software. The created file was viewed from an ASCII text editing program by excel spreadsheet and the same downloading procedure was used to retrieve the electromagnetic and radiometric field data.

2.5 Radiometric ternary image

A ternary radiometric image was plotted using the four grid channels from Oasis Montaj, which includes; the potassium, uranium, thorium and the total count. Three apexes were used to depict compositions of uranium (yellow), potassium (blue) and thorium (red) and allows comparison between uranium, potassium and thorium at once, every position or point on the ternary plot represents a different composition of the three elements. The radiometric ternary image also assists in distinguishing between different lithologies as shown by variations in colour which is due to the different mineral abundances of potassium, uranium and thorium. Distinguishing between the different lithologies may be difficult when image becomes saturated (all abundances are relatively high) and where images becomes very dark, which is believed to be due to low abundances of the radioactive elements, the sum of the variables (elements) is taken to be a constant which is represented as 1.0 or 100%. Element ratio maps were also produced i.e. $\text{K}/\text{K}+\text{U}+\text{Th}$, $\text{U}/\text{K}+\text{U}+\text{Th}$, $\text{Th}/\text{K}+\text{U}+\text{Th}$.

III. RESULTS AND DISCUSSION

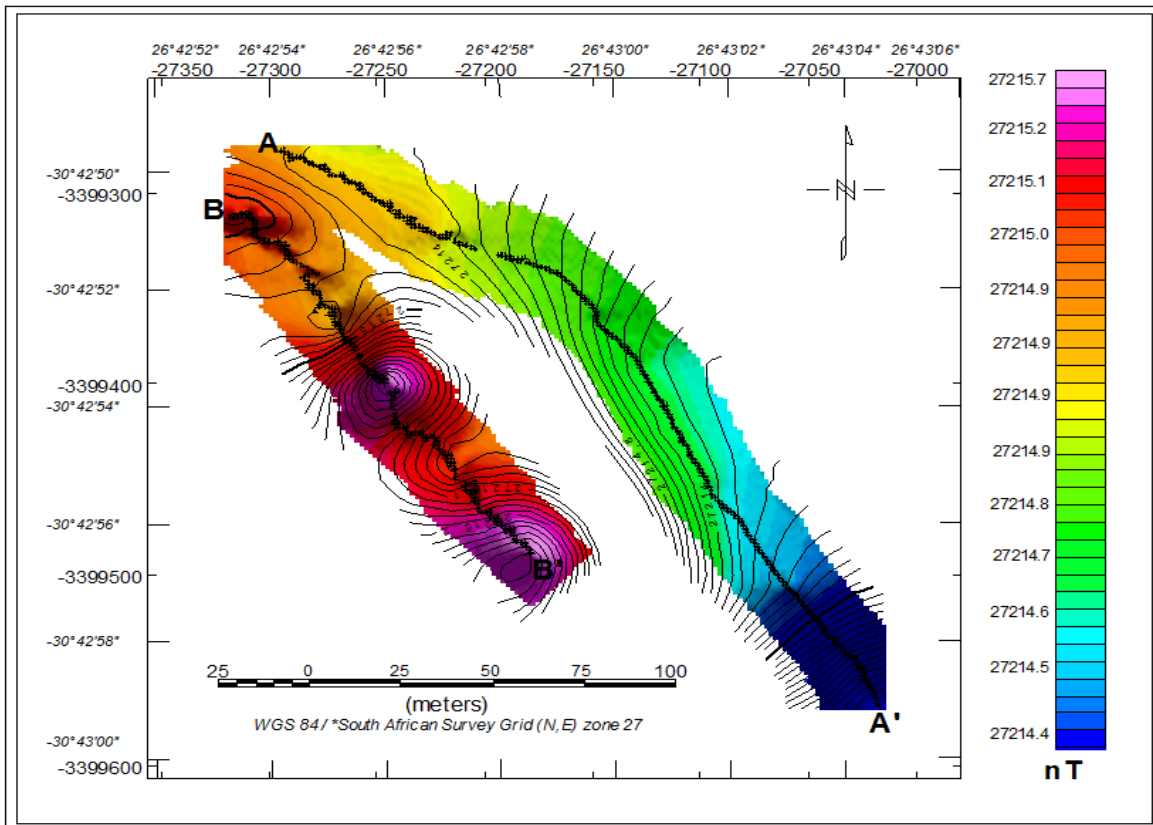


Figure 5 Total magnetic field map of Aliwal North spa. Two main areas of high magnetic field are seen in the map and they both lie along Line 2 (B - B') and falls within 3399400 E to 3399500 E and 27150 S to 27250 S on the magnetic map.

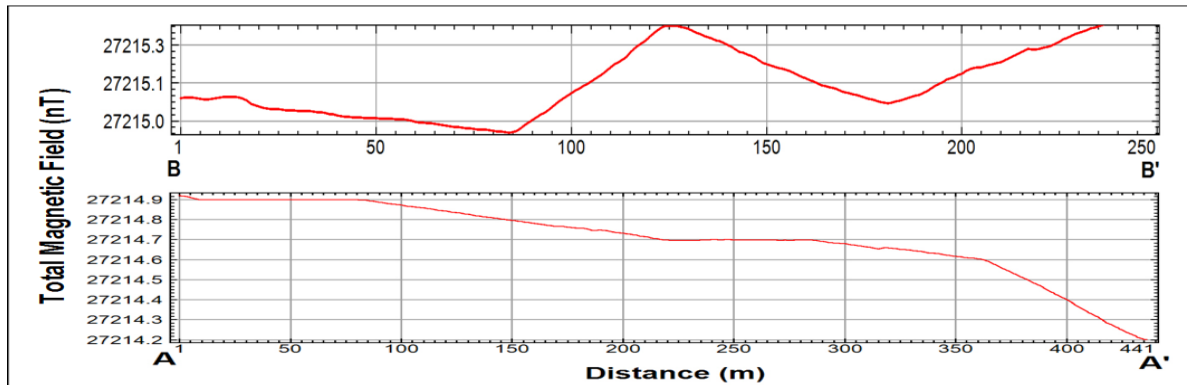


Figure 6 Profile for total magnetic field for Line 1 and Line 2.

Figure 6 shows a total magnetic field of 27215.3 nT on the northwestern side of the survey site along Line 1 (A - A') which remains constant for a distance of about 85 m and thereafter decreases slowly to a value of 27214.9 nT at the end of the line. The magnetic field along Line 2 (B - B') in the northwestern side of the map is about 27215.03 nT and decreases gradually to 27214.9 nT at a distance of about 85 m. It increases continuously from 27214.9 nT at a distance of 85 m until a peak of 27215.28 nT was reached at a distance of about 130 m, then decreases gradually to 27215.02 nT at a distance of about 190 m and further increases continuously until a total magnetic field of 27215.3 nT was reached at the end of the line. The observed anomaly along Line 2 (B - B') with amplitude of about 0.4 nT could be a real feature extending to depth. No discernable contrast was observed on the Line 1 (A - A').

Table 2 The nominal exploration depths for three coil spacing with the horizontal and vertical dipole orientation using EM34-3 (Modified from www.nga.com/Flyers PDF/NGA).

Coil separation (m)	Nominal depth-VD (m)	Nominal depth- HD (m)
10	14.2	6.8
20	28.6	13.5
40	57	29

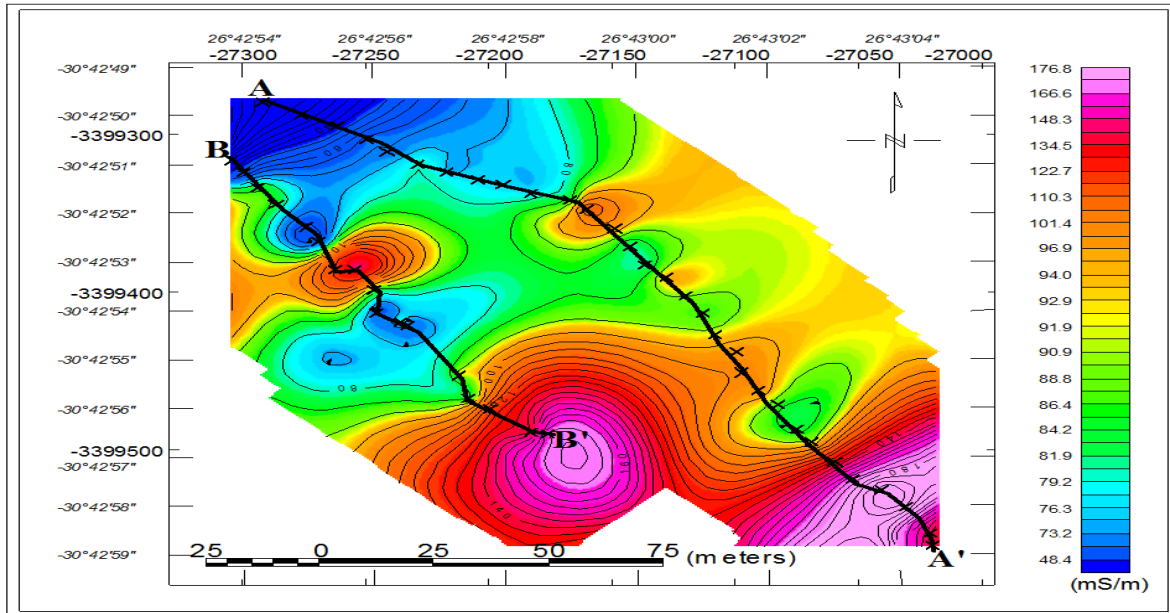


Figure 7 EM conductivity map for Line 1 and Line 2 (10 m coil separation). Two major zones of high conductive zones are seen in the map extending to a depth of about 10 m, the first conductive zone fall within 3399450 E to 3399550 E and 27150 S to 27200 S on the EM map which lies along Line 2 and the second anomaly is observed on the southeastern (SE) side of the map along Line 1. The conductive bodies occur at a depth of 7.5 m.

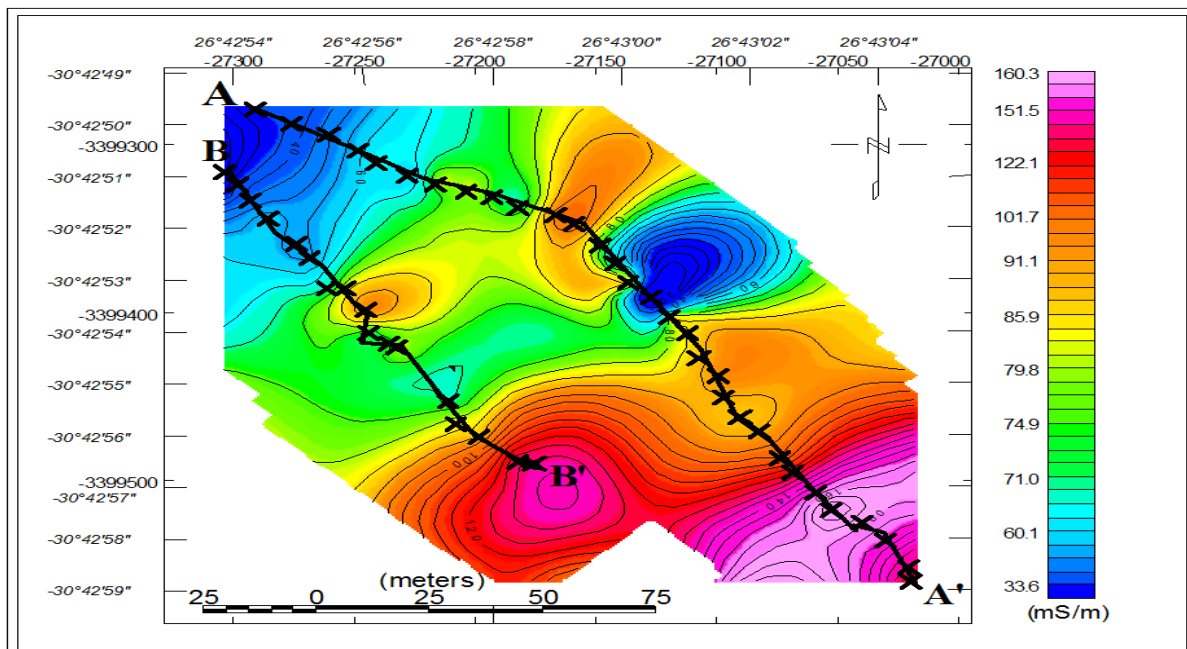


Figure 8 EM conductivity map for Line 1 and Line 2 (20 m coil separation). Two high conductive zones are seen in map extending to depth of about 20 m, the first conductive zone lies within 3399450 E to 3399550 E and 27150 S to 27200 S on the map and the second zone is seen on the southeast side of Line 1 on the map. The conductive bodies occur at a depth of 15 m.

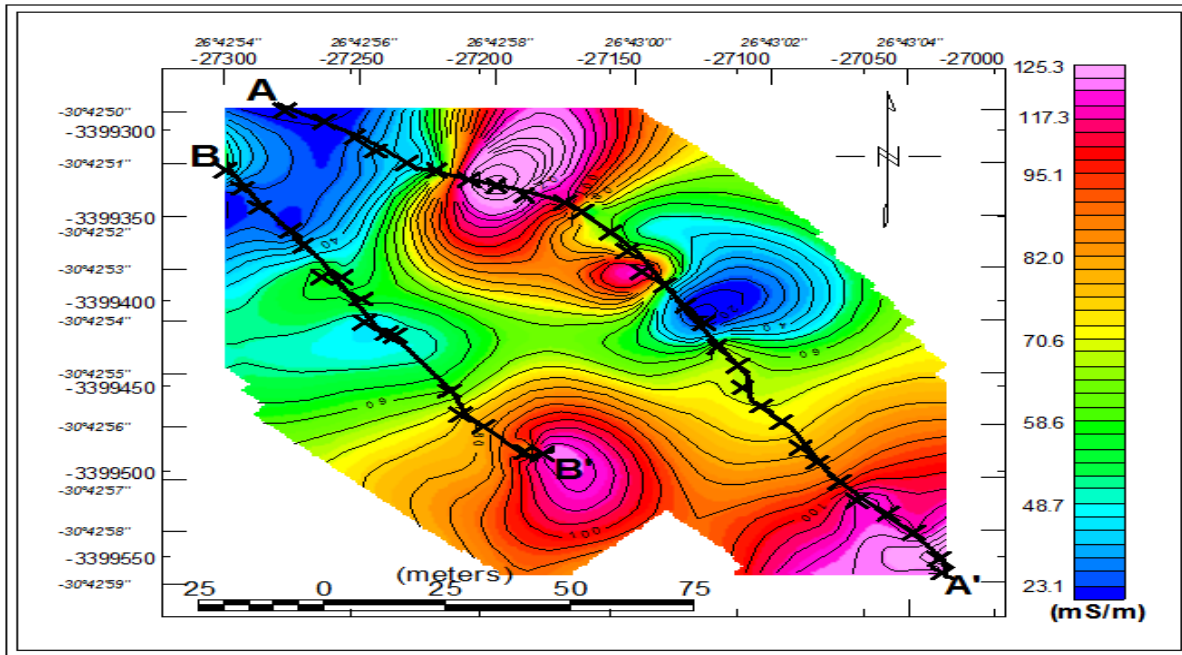


Figure 9 EM conductivity map for Line 1 and Line 2 (40 m coil separation). Three high conductive zones is seen in the map extending to a depth of about 30 m, the first conductive zone lies within 3399300 E to 3399350 E and 27150 S to 27200 S, the second anomaly occurs within 3399450 E to 3399550 E and 27150 S to 27200 S and the third anomaly lies in the southeastern part of the map. The first and second anomalies were along Line 2 while the third anomaly falls on Line 1.

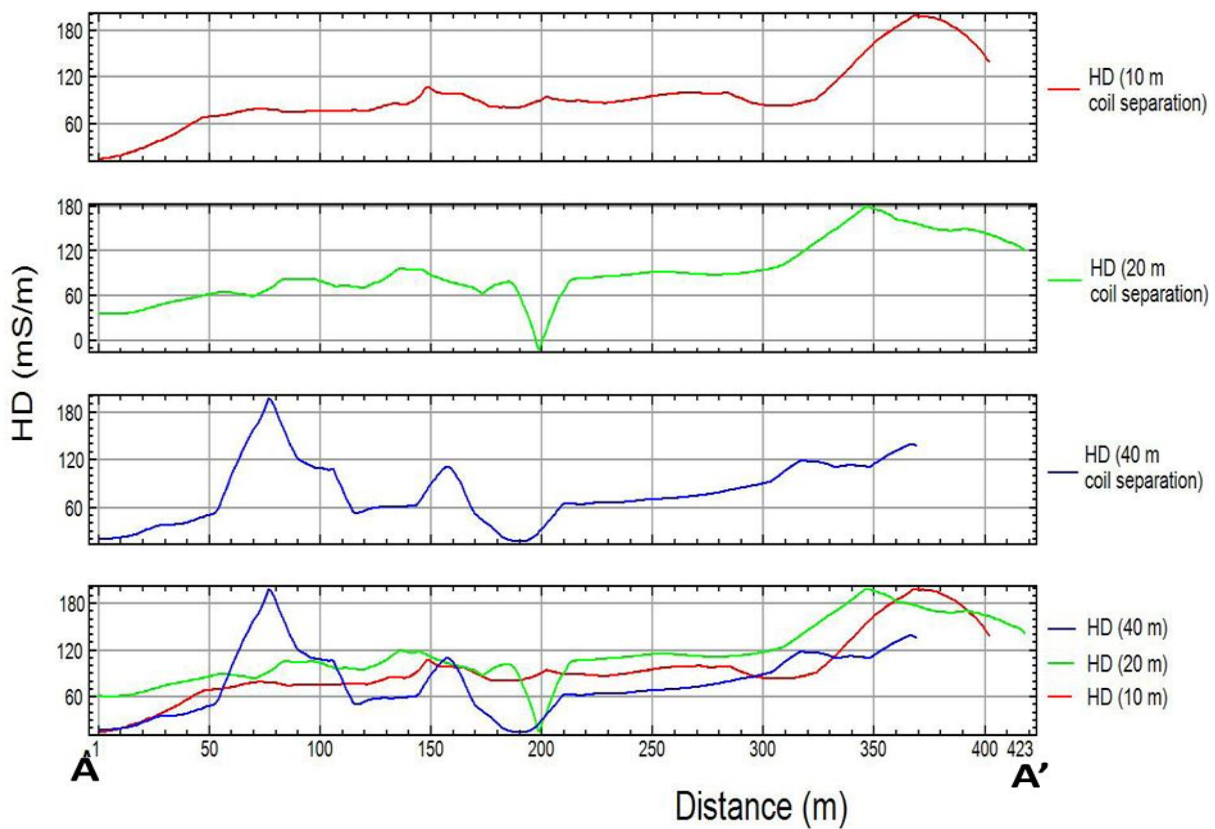


Figure 10 EM combined profiles for Line 1 (10 m, 20 m and 40 m coil separation).

Figure 10 shows two main conductive zones along Line 1 (A –A’), the first anomaly was picked up using the 40 m coil separation which indicates that a conductive body occur at a depth of about 30 m in the

ground between distances of 55 m to 110 m but disappears at shallow depth (7.5 m). The conductive body that was picked up using the 10 m and 20 m coil separations (55 m to 110 m) could be due to near surface effect. The second conductive body was picked up using the 10 m, 20 m and 40 m coil separations between distance of about 300 m to 423 m, indicating that the conductive body occur at shallow depth (7.5m) and extends to deeper depth (30 m). This body could be dolerite intrusion occurring at depth with associated faulting.

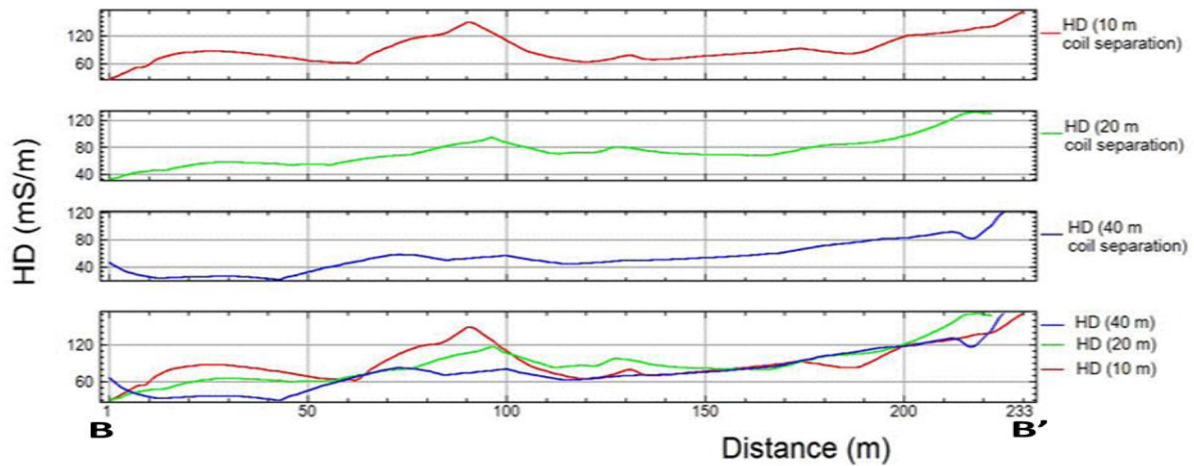


Figure 11 EM combined profiles for Line 2 (10 m, 20 m and 40 m coil separation).

Figure 11 shows that an anomaly (conductive body) was picked up using the 10 m, 20 m and 40 m coil separation between the distance of 190 m to 223 m, this conductive body is not just due to near surface effects like overburden but continues to a depth of up to 30 m into the ground. The second conductive body was picked up using the 10 m and 20 m coil separation between the distances of about 57 m to 120 m. This conductive body occurs up to a depth of 15 m but disappears at 30 m which could be due to near the surface effect.

Table 2 Classification for radioactive elements measurement (Baiyegunhi, 2012).

Measurements	Low	Moderate	High	Very high
Dose count (nSv/hr)	≤ 19	20-39	40-59	≥60
Relative Abundance (%)	≤19	20-39	40-59	≥60
Count (cpm)	≤19	20-39	40-59	≥60
Count (ppm)	≤0.10	0.11-0.79	0.8-1.49	≥1.5

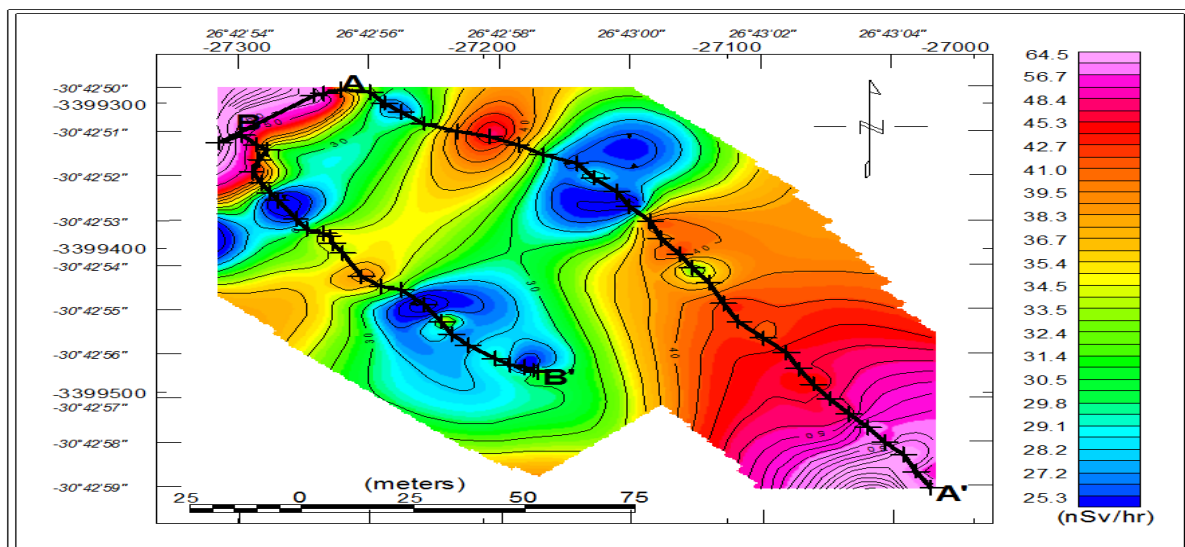


Figure 12 Total count map, also showing profile Line 1 and Line 2. Line 1 cut the high total count zone in the southeastern side and the high total count zone in the northwestern side of the map was slightly cuts by both Line 1 and 2.

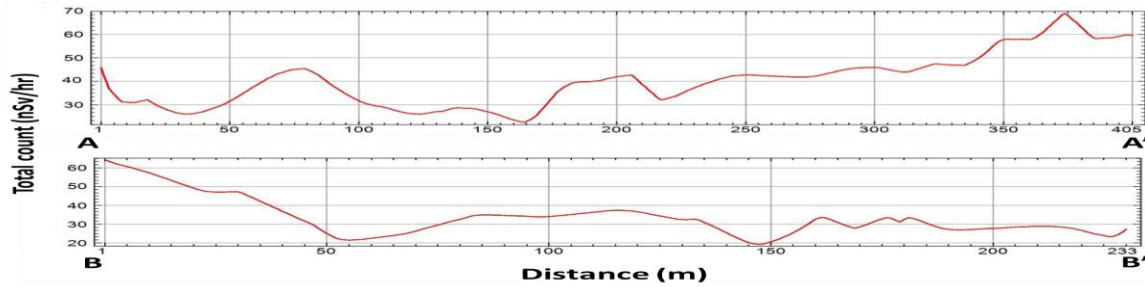


Figure 13 Profile for Total Count (nSv/hr) along Line 1(A - A') and Line 2 (B - B'). The profile indicates a relatively high dose count of around 46 nSv/hr at the start of Line 1, which decreases to 25 nSv/hr at a distance of approximately 45 m and gradually increases up to 46 nSv/hr at distance of about 90 m. The dose count further decreases to about 5 nSv/hr and gradually increases to 60 nSv/hr at the end of the Line 1. High dose count of about 64 nSv/hr is seen at the start of Line 2, which slightly decreases to 22 nSv/hr at a distance of around 55 m and gradually increases to 35 nSv/hr at a distance of about 82 m. The dose count further increases and decreases until the end of the line was reached. The areas of high dose count in the map are believed to be associated with the intrusion of dolerites as well as radioactive elements like uranium and thorium in the detrital materials.

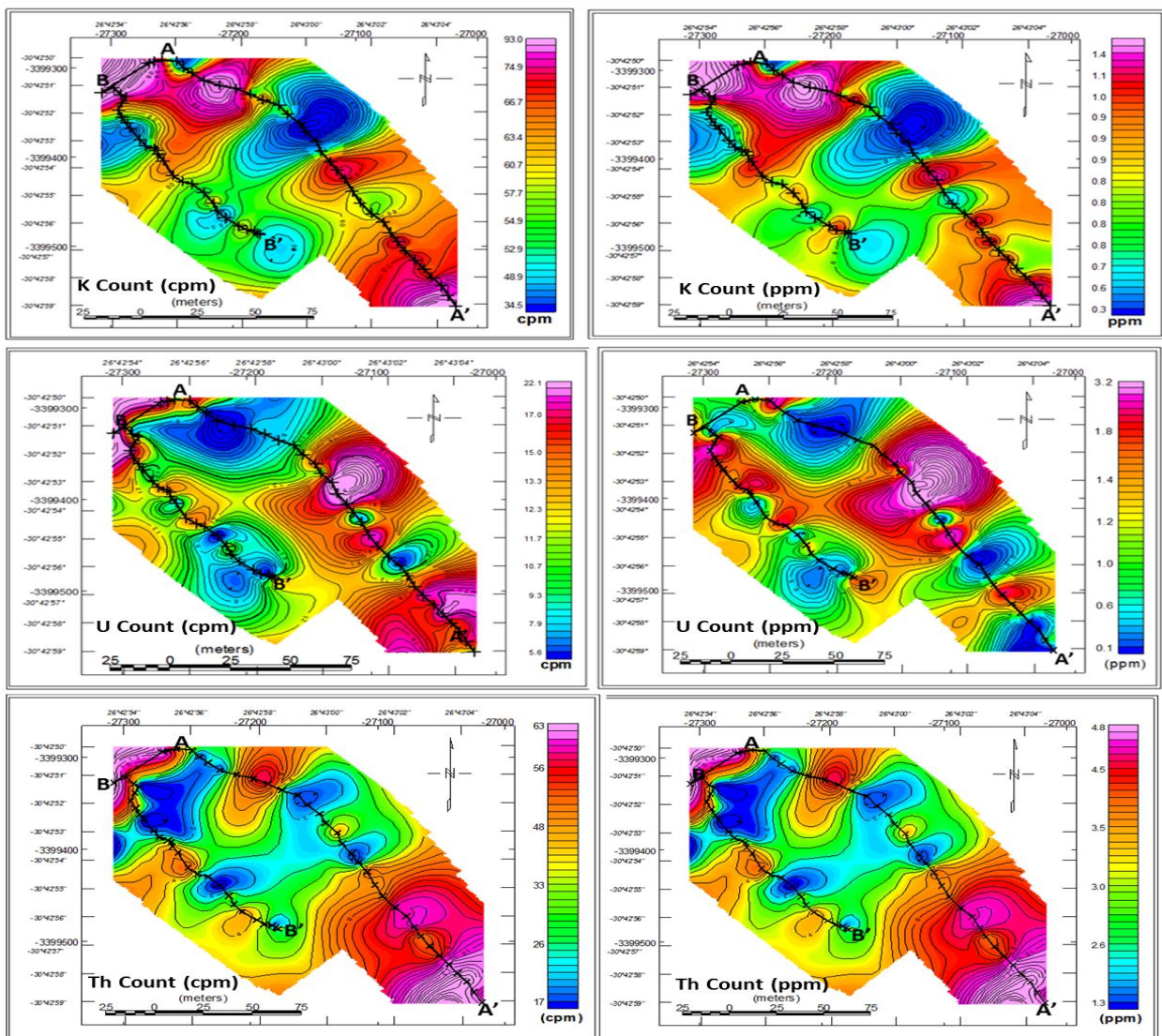


Figure 14 Map showing potassium, uranium and thorium count in cpm and ppm along Line 1 and 2. Generally, there are high radioactive elements along Line 1, although, the concentration and location of each element varies along the profiles. For instance, along Line 1, potassium and thorium are seen to be high at the start and towards the end of the profile, while uranium is high at half-way through Line 1 (A - A'). Radioactive count is relatively low and varies along Line 2 (B - B').

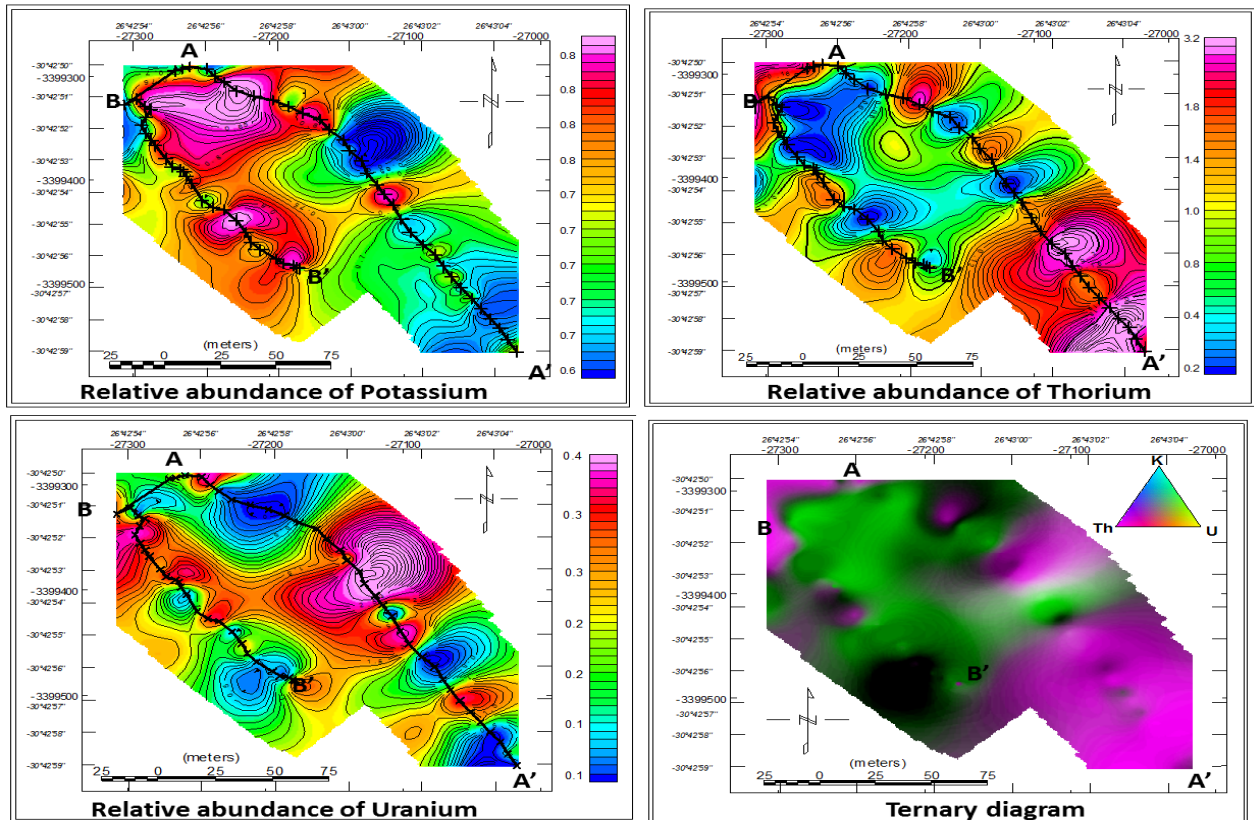


Figure 15 Ternary diagram and relative abundance of potassium, uranium and thorium.

Generally, there is high abundance of radioactive elements (U, K and Th) along Line 1. Figure 15 shows that the northwestern side of the survey site is enriched in thorium (dominant in the southeastern side). Uranium is more prominent in northeastern part, while potassium is more in the northwest part in contact with the thorium. The ternary image shows NW- SE trending linear feature underlying the survey site which could be the source of other minor trends in the area, this linear trends are assumed to be faulting that is associated with the intrusion of the Karoo dolerites. From the ternary diagram, it can be inferred that thorium is the most abundance radioelements in the study area.

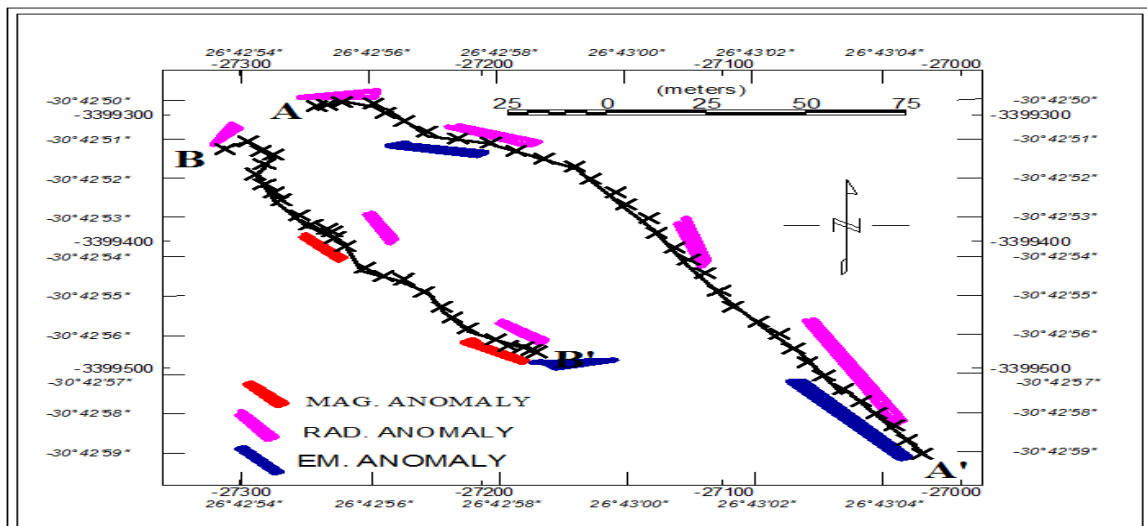


Figure 16 Interpretation map for Line 1 and Line 2.

Figure 16 shows that the EM and gamma ray anomaly between the distances of 300 m to 420 m along Line 1 in the southeastern part of the map, and they both coincide or agree. This anomaly is the major anomaly in the survey area which occurs at shallow depth, as well as extends to depth of about 30 m. It is suggested that the anomaly might be dolerite intrusions at depth with associated faulting. The EM and gamma ray anomaly also

agrees in the north-northwestern side of the map along Line 1 between the distances of 50 m to 120 m, although this anomaly occurs to a depth of about 30 m but disappears at shallow depth. The magnetic, EM and gamma ray survey anomaly coincides along Line 2 within 180 m to 233 m and occur at a depth of 30 m. The second anomaly was picked between the distance of 50 m to 120 m by the magnetic and gamma ray survey, this anomaly that appears at shallow depth and disappears at greater depth could be due to near surface effects.

The magnetic data for Line 1 shows no discernable contrast while that for Line 2 shows a relatively low amplitude or change in the magnetic field with amplitude of about 0.4 nT, which could be a real feature possibly at great depth.

The combined EM result along Line 1 (Figure 10) signifies the existence of conductive body between the distances of about 330 m to 408 m. This buried body was picked up when using 10 m and 20 m coil separations indicating that the body is not just due to near surface material effect but extends deeper, which could possibly be due to dolerites in the form of sills and dykes at depth. The 40 m coil separation also picked a conductive body that occurs at a nominal depth of about 30 m in the ground between a distance of 60 m to 120 m (along Line 1) which disappears at a distance of about 215 m, another conductive body at a distance of 330 m to 374 m was detected which coincides with the conductive body that was picked up by the 10 m and 20 m coil separation, respectively. The EM combined results (Figure 11) along Line 2 shows a conductive body that was picked up when using the 10 m and 20 m coil separations indicating that the conductive body is not just due to near surface effect like overburden but continues to a nominal depth of up to 15 m. The 40 m coil separation also indicates that the conductive body continues to a depth of about 30 m into the ground. The gamma ray results indicate a high concentration of the three radioactive elements (K, U, and Th) in the Aliwal North spa. The high concentration of these radioactive elements could be due to high radioactivity which may be associated with the intrusions such as dolerite dykes along the fractured and fault zones.

The presence of hot springs in a locality, such as Aliwal North can be linked to the presence of deep structures, neotectonic zones (e.g. fault-zones) that provide support to the circulation of convectional currents as well as artesian systems (Kent, 1969). Presently, three neotectonic belts (southern, eastern and northern belts) are documented in the Eastern Cape Province (Figure 2). From the rocks of the Cape Fold Belt, the southern neotectonic belt extends to the rocks of the Adelaide Subgroup in the Beaufort Group (Madi, 2013). Madi (2013) further explained that, out of the twelve (12) hot springs situated in the Eastern Cape, seven (7) of hot springs are located within the northern neotectonic belt. The existence of the seven (7) hot springs in neotectonics zone also agrees with the suggestion that hot springs are possible indicator of neotectonics. Based on this explanation, Maud *et al.* (1983) concluded that the 1983 basaltic eruption in Lesotho can be attributed to ascension or upwelling of magma in the area that led to the heating of the underneath water.

Uranium deposits in the Karoo Supergroup are confined to fluvially-deposited sandstones in the Adelaide Subgroup. Cole and Wipplinger (2001) stated that the absence of uranium in lithologies of similar disposition in terms of depositional environment (paleoclimate and palaeoenvironments) is probably due to the absence or lack of a suitable uranium source at the time of metallogenesis. Basement granite has been proposed as possible uranium sources for the Adelaide and Tarkastad Subgroups. The warm, semi-arid paleoclimate of all these stratigraphic units (Beaufort Group) signifies an oxidising environment, which is required for the leaching and mobilisation of uranium from the above sources. Solutions containing radioactive elements like uranium-bearing solutions probably migrated through the sand bodies with precipitation occurring in relatively sparse reduced zones that contained carbonaceous debris that are deposited in the Aliwal North hot spring. The radiometric result reveals that thorium is the most abundant in the study area and their concentration is less than the world average hazardous threshold (7.4 ppm). This result also agrees with the work of several authors (e.g. Hartnady, 1985; Oliver *et al.*, 2011; Madi, 2010; 2014) that study the hot springs in the South Africa. They allude that the concentration of the radioactive elements (U, K and Th) is relatively low and acceptable for groundwater (hot springs) consumption based on the concentration of radioactive elements; however, it could be harmful to humans' health, as well as animals when exposed to the radiation or consumed over a long period of time.

IV. CONCLUSIONS

Based on the results presented in this paper, the following conclusions are made:

- Most of the anomalies are suggested to be dolerite intrusion with associated faulting that runs in a south-westerly to north-easterly direction, although few anomalies show south-easterly to north-westerly direction.
- The results for EM Line 1 and Line 2 where high conductivity bodies (≥ 80 mS/m) were detected could be due to the intrusions such as dolerite dykes along the fractured and fault zones, while moderate (65 - 79 mS/m) and low (≤ 64 mS/m) conductivities areas may be related to near surface mineralization in the argillaceous sedimentary rocks (red mudstone, light grey sandstone and grey shale) of the Tarkastad Subgroup which was intruded by the dolerite dykes.

- It was inferred that Aliwal hot spring is of meteoric origin and the source of the heat is due to the deep circulation along the major fault zones through which the water percolates into the ground and gets to a deeper depth.
- The radiometric ternary and relative abundance maps reveal that thorium is the most abundant radioactive element in the area.
- From the gamma radiation count maps (cpm and ppm), it could be deduced that region with high gamma radiation count could be due to the uranium and thorium in the detrital material, as well as the accumulation of radioelements in the sediments of the Tarkastad Subgroup that are rich in feldspars (K-feldspar) with calcite, quartz and clay minerals. The radioactive elements are believed to be sourced from the fluvial sandstone, surrounding shales and probably the Precambrian basement granites.

It is recommended that detailed geological mapping and geophysical surveys with a reduced line spacing (5 m) should be carried out to determine the extent and concentration of the minerals present in the area whereby the full economic potential of Aliwal thermal spring can be achieved, which could be a substantial economic contribution to the local area and the country's economy at large. It is also recommended that a regular geochemical sampling and analysis should be carried out on the water samples and the responsible authorities should be informed of the potential health hazards that are related to the long-term consumption of the untreated thermal water which may contain dissolved minerals and the general public in the area should be alert of the risks, control and treatment measures. It is strongly recommended that substitute or alternative source of portable water should be provided and the thermal spring environmental and economic potentials should be maximised.

V. CONFLICT OF INTERESTS

The authors declare that there is no conflict of interests regarding the publication of this paper.

VI. ACKNOWLEDGMENTS

The authors thank Govan Mbeki Research and Development Centre (GMRDC) for supervisory link bursary. Mr Peter Nyabeze and Mr Matome Sekibi of the Council for Geoscience are kindly appreciated for the logistics as well as providing geophysical instruments for the field work.

REFERENCES

- [1] Adele, M., (1994). Geophysical methods in geothermal exploration. Italian National Research Council International Institute for Geothermal Research Pisa, Italy.
- [2] Baiyegunhi, C., (2012). Geophysical investigation of Aliwal North Spa in the Eastern Cape, South Africa. Honours Project, University of Fort Hare. P.1-60.
- [3] Boekstein, M., (1998). Hot Springs Holidays: Visitors' Guide to Hot Springs and Mineral Spa Resorts in Southern Africa. Mark Boekstein and Logo Print, Cape Town.
- [4] Catuneanu, O., and Elango, H.N., (2001). Tectonic control on fluvial styles: the Balfour Formation of the Karoo Basin, South Africa. *Sedimentary Geology*. vol. 140, p. 291- 313.
- [5] Cole, D.I. and Wipflinger, P.E., (2001). Sedimentology and molybdenum potential of the Beaufort in the main Karoo Basin, South Africa. *Memoir, Council for Geoscience*, vol. 80, p 1-225.
- [6] Donald B., Douglas P. K., and David C. C., (1992). Geophysical methods in exploration and mineral environmental investigations. *Society of Exploration Geophysicists*. p. 1-9.
- [7] EM34-3 and EM34-3XL Operating instructions for model with two digital meters (2007). Geonics Limited.
- [8] EM34-3 and EM34-3XL Operating Instructions (1994). Geonics Limited.
- [9] Hancox, P.J. and Rubidge, B.S., (2001). Breakthroughs in the biodiversity, biogeography, biostratigraphy and basin analysis of the Beaufort Group. *African Earth Sciences*, vol. 33, p 563-577.
- [10] Hardy, C. C., (2005). Characterizing thermal features from multi-spectral remote sensing data using dynamic calibration procedures [Ph.D. dissertation]: University of Montana at Missoula, p. 124-153.
- [11] Hartnady, C.J. (1985). Uplift, faulting seismicity, thermal spring and possible incipient volcanic activity in the Lesotho-Natal region, SE Africa: the Quathlamba hotspot hypothesis. *Tectonics* 4, p. 371-377.
- [12] Hobday, D.K., (1973). Middle Ecca deltaic deposits in the Muden-Tugela Ferry area of Natal. *Transactional Geological Society of South Africa*, vol. 76, p 309-318.
- [13] Johnson, M. R., (1976). Stratigraphy and sedimentology of the Cape and Karoo sequences in the Eastern Cape Province. PhD Thesis (unpublished), Department of Geology, Rhodes University, Grahamstown.
- [14] Kent L. E., (1949). The thermal waters of the Union of South Africa and South West Africa. *Trans. Geol. Soc. S. Afr.* 52 231-264.
- [15] Kent L. E., (1969). The thermal waters in the Republic of South Africa. In: Proc. Of Symposium II on mineral and thermal waters of the world, B-overseas countries, Vol. 19, Report of the 23rd session of the International Geological Conference, 1968, Academia, Prague, 143-164. *Developments in Geophysical Exploration. Methods – 2*. Applied Science Pub., p. 107-150.
- [16] Madi, K., (2010). Neotectonics and its applications for the exploration of groundwater in the fractured Karoo aquifers in the Eastern Cape, South Africa. MSc thesis, University of Fort Hare. p. 12-160.
- [17] Madi, K., Nyabeze P., Gwavava, O., Sekiba, M and Zhao, B., (2014). Uranium, thorium and potassium occurrences in the vicinity of hot springs in the northern neotectonic belt in the Eastern Cape Province, South Africa. *J Radioanal Nucl Chem.*, 301:351-363. DOI 10.1007/s10967-014-3183-1.
- [18] MagMap 2000 (24891-01 Rev. G). User Guide Geometrics Inc.

- [19] Maud, R., Partridge, T. C., and Dunleavy, J., (1998) The Lesotho “volcanic” event of 1983. *South Afr J Geol* 101(4):313
- [20] Olivier, J., Venter, J. S and Jonker, C. Z., (2008). Thermal and chemical characteristics of thermal spring in the northern part of the Limpopo Province, South Africa, *Water SA* 34 (2) 163-174.
- [21] Oliver, J., Venter, J.S and Jonker, C.Z., (2011). Thermal and chemical characteristics of hot springs in the northern part of the Limpopo Province, South Africa. Available on line <http://www.wrc.org.za>
- [22] Rubidge BS. (2005). Re-uniting lost continents – Fossil reptiles from the ancient Karoo and their wanderlust. *S Afr J Geol.*v.108, p135–172. <http://dx.doi.org/10.2113/108.1.135>
- [23] SACS, South African Committee for Stratigraphy, (1980). Stratigraphy of South Africa. Part 1: Lithostratigraphy of the Republic of South Africa, South West Africa/Namibia and the Republics of Bophuthatswana, Transkei and Venda (Compiled by Kent, L.E.). Geological Survey of South Africa. Handbook, 8, 690pp.
- [24] Scintrex, (1996). Magnetic Applications Guide. Scintrex Limited.
- [25] Tordiffe, E. A. W., (1978). Aspects of the hydro-geochemistry of the Karoo Sequence in the Great Fish River Basin Eastern Cape Province: With special reference to the groundwater quality. Ph.D. thesis (unpubl.). Univ. O.F.S., Bloemfontein, 307pp.
- [26] Visser, J.N.J. and Dukas, B.A., (1979). Upward fining fluvial megacycles in the Beaufort Group, north of Graaff-Reinet, Cape Province. *Trans. Geol. Soc. S. Afr.*, vol. 82, p 149-154.
- [27] Visser, D.J.L., Gordon, J.F., and Venter, C.P., (1984). Geological map of the Republic of South Africa, Transkei, Bophuthatswana, Venda and Ciskei, and the Kingdoms of Lesotho and Swaziland: Gravity edition, Geol. Surv. Rep. South Africa, Pretoria.
- [28] Yibas, B., Olivier, J., Tekere, M., Motlakeng, T and Jonker, C. Z., (2011). Preliminary Health Risk Analysis of Thermal Springs In Limpopo Province, South Africa based on water Chemistry. Proceedings, Kenya Geothermal Conference.